PERGAMON

International Journal of Solids and Structures 39 (2002) 1119–1130

INTERNATIONAL JOURNAL OF SOLIDS and STRUCTURES

www.elsevier.com/locate/ijsolstr

Wave propagation in piezoelectric coupled plates by use of interdigital transducer Part 1. Dispersion characteristics

Q. Wang [a,*], V.K. Varadan [b]

[a] *Department of Civil Engineering, National University of Singapore, Block E1A, #07-03, 1 Engineering Drive 2, Singapore 117576, Singapore*

[b] *Department of Engineering Science and Mechanics, The Pennsylvania State University, University Park, PA 16802, USA*

Received 23 May 2001

Abstract

In the first part of this research paper on SH wave propagation in the piezoelectric coupled plate by use of interdigital transducer (IDT), the dispersion characteristics and the mode shapes of the wave propagation in this structure are presented. The piezoelectric coupled plate is made of a metal host plate and a piezoelectric layer surface bonded on the metal substrate. Such structure is analysed with piezoelectric effects fully coupled for the purpose of applying IDT to the health monitoring of structures. The mathematical model of the SH wave propagation in this plate structure is based on the type of surface wave solution. From the numerical simulations, the Bleustein–Gulyayev surface wave is observed for the first mode of the wave propagation in this paper. The asymptotic solution for higher modes is the shear velocity of the piezoelectric layer. The comparison of the dispersion curves for this piezoelectric coupled plate and the semi-infinite piezoelectric coupled medium is also conducted. The mode shapes of the deflection and the electric potential of the piezoelectric layer are derived and discussed. This research provides the basic model for the analysis of the wave propagation in piezoelectric coupled plate, and the excitation of this type of surface wave by use of IDT will be studied in the second part of the research.

Keywords: Piezoelectric coupled plate; Interdigital transducer; Dispersion characteristics; Wave phase velocity; Health monitoring of structures

1. Introduction

Interdigital transducer (IDT) was first used to excite the surface wave (SAW) devices in radar communication equipment as filters and delay lines (Varadan and Varadan, 2000), and some consumer areas such as pagers, mobile phone, and sensors (Morgan, 1998; Campbell, 1998; White, 1998). Its applications in separating, amplifying, and storing signals and in other signal processing applications in acoustoelectronics

* Corresponding author. Tel.: +65-874-4683; fax: +65-779-1635.
E-mail address: cvewangq@nus.edu.sg (Q. Wang).

0020-7683/02/$ - see front matter
PII: S0020-7683(01)00243-8

were also considered important (Auld, 1973a,b; Parton and Kudryavtser, 1988). It should be noted in these applications that, a semi-infinite piezoelectric medium was usually used as the substrate surface bonded by a layer of metal. The dispersive characteristics of wave propagation in the above structures are main topics to be studied before the application of IDT in wave excitation was conducted. Curtis and Redwood (1973) proposed a solution for dispersion characteristics of the SH wave in a piezoelectric material of class 6 mm. The conditions for the existence of various modes were presented. The piezoelectric medium in their studies was surface bonded by a layer of metal. Such device was mainly used in geophysics and ultrasonics for the processing of electrical signals. Hanhua and Xingjiao (1991, 1993) and Kielczynski et al. (1989) further provided analyses on the shear-horizontal surface waves on piezoelectric ceramics with metal surface layer. Their studies again presented the conditions for the existence of B–G surface wave and discussed a new surface wave in the piezoelectric structure. To achieve desirable dispersion behaviour of elastic wave in designing time delay device, Sun and Cheng (1974) introduced a metallic film overlay to a piezoelectric cylinder. Different metal materials were employed to compare the coupling effect of different metal layers. The review of the excitation of these waves by use of IDT will be discussed by the second part of the paper. A general conclusion of the research on wave excitation by use of IDT is that an accurate analytical solution for the wave excitation is expected.

IDT is recently found to have great potentials to be used as attractive sensors for various physical variables, such as force, electric fields, magnetic fields, temperature, pressure and etc. (Varadan and Varadan, 2000). Nowadays, an important application field of IDT is in the health monitoring of structures. Some methods and experimental works on the rapid monitoring of structures using IDT to excite Lamb wave have been attempted (Badcock and Birt, 2000; Monkhouse et al., 2000). A premise of applying IDT in the wave excitation in the health monitoring of structures is to obtain the wave dispersion characteristics of the piezoelectric coupled structures consisting of the substrate, mainly referred to metals and composites, and a layer of piezoelectric materials. The new application of IDT in health monitoring of structures initialises challenges in the field of structural mechanics. Since IDT is bonded on a piezoelectric layer which is surface bonded on the metal substrate, the piezoelectric effects must be modelled in the dispersion characteristics of the piezoelectric coupled structure. Such piezoelectric effect makes the physical model more complicated in both the derivation of the dispersion characteristics and the derivation of the mathematical solution of the wave excitation by IDT. An accurate model coupling the piezoelectric effect in a piezoelectric coupled structure is a key to study wave propagations in the structure. Wang et al. (2001) studied the Love wave propagation in a semi-infinite metal medium with a piezoelectric layer mounted on the surface. The Bleustein–Gulyaev wave was observed for the first mode of the wave solution. Some other wave modes were also observed. The mode shapes of the electric potential and displacement were studied as well in their work. However, more researches to further explore the potential of IDT in health monitoring of structures are necessary.

The objective of this paper is to study the SH wave propagation in the piezoelectric plate. The dispersive characteristics of wave propagation and the mode shape of the displacement, the electric potential, and the electric displacement will be discussed in the first part of the research paper. An analytical solution for the excitation of this type of surface wave by use of IDT is to be studied in the second part of the paper.

2. Formulation of the problem

Consider a metal plate with thickness h' surface bonded by a layer of piezoelectric material with thickness h as illustrated in Fig. 1. The propagation of SH wave in the host metal medium is governed by

$$c'_{44}\nabla^2 u'_3 = \rho' \frac{\partial^2 u'_3}{\partial t^2} \tag{1}$$

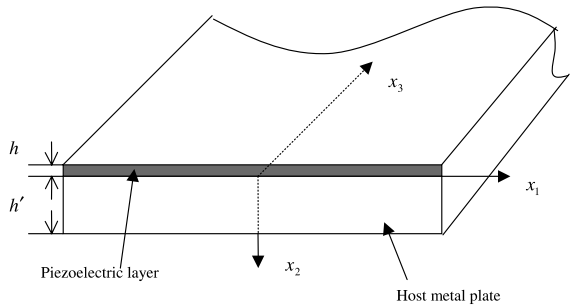

Fig. 1. An infinite metal plate surface bonded by a layer of piezoelectric material.

where $c'_{44} = 2G = E/(1+\nu')$ is the shear modulus, ρ' the mass density, ν' the Poisson ratio, E the Young's module of the host medium, u'_3 the deflection of the host medium in the x_3 direction, and ∇^2 the Laplace operator given by $\nabla^2 = \partial^2/\partial x_1^2 + \partial^2/\partial x_2^2$.

The shear stress can be written as

$$\sigma'_{23} = c'_{44}\frac{\partial u'_3}{\partial x_2} \tag{2}$$

When the poling direction of the piezoelectric layer is the transverse x_3-direction, the coupling equation for the piezoelectric layer is (Viktorov, 1981).

$$c_{44}\nabla^2 u_3 + e_{15}\nabla^2\phi = \rho\frac{\partial^2 u_3}{\partial t^2} \tag{3}$$

$$e_{15}\nabla^2 u_3 - \Xi_{11}\nabla^2\phi = 0 \tag{4}$$

where $c_{44} = (c_{11} - c_{22})/2$ is the elastic modulus, e_{15} the piezoelectric coefficient, Ξ_{11} the dielectric constant, and ρ the mass density of the piezoelectric layer, u_3 the deflection of the piezoelectric layer in the x_3-direction, and ϕ the electric potential. The shear stress in the piezoelectric layer is then written as

$$\sigma_{23} = c_{44}\frac{\partial u_3}{\partial x_2} + e_{15}\frac{\partial\phi}{\partial x_2} \tag{5}$$

Considering the case when the electrodes on the surfaces of the piezoelectric layer are shortly connected, the boundary conditions for this piezoelectric coupled plate structure are expressed as

at $x_2 = 0$:

$$u_3 = u'_3 \tag{6}$$

$$\sigma_{23} = \sigma'_{23} \tag{7}$$

$$\phi = 0 \tag{8}$$

at $x_2 = -h$:

$$\sigma_{23} = 0 \tag{9}$$

$$\phi = 0 \tag{10}$$

at $x_2 = h'$:

$$\sigma'_{23} = 0 \tag{11}$$

The solutions of u_3' for wave propagation in the x_1-direction can be expressed as

$$u_3' = f'(x_2)e^{i\omega(t-(x_1/c))} \tag{12}$$

Substituting Eq. (12) into Eq. (1) yields the solution of u_3' as

$$u_3' = (C_1e^{-\chi' x_2} + C_2e^{\chi' x_2})e^{i\omega(t-(x_1/c))} \tag{13}$$

where $\chi' = \omega/c\sqrt{1-(c/v')^2}$, $v'^2 = c_{44}'/\rho'$, and the derivation of Eq. (13) is under the assumption of $c < v'$. It can be seen from Eq. (13) that the wave decays exponentially in the thickness direction of the plate. As such, we refer this type of the solution of the wave propagation as the surface wave solution. Such surface wave solution will not exist when SH wave in a pure metal layer in considered. When $c > v'$, the SH wave propagation in a pure metal layer is studied by Graff (1975) by using the type of plane wave solution which uses the sine and cosine functions to present the wave solution in the flexural direction of the plate. In this paper, the type of surface wave solution of the SH wave propagation in the piezoelectric plate based on Eq. (13) will be discussed in the first part of the paper. Further, this type of surface wave solution will be used in the deduction of the surface wave propagation by use of IDT in this piezoelectric coupled plate in the second part of the paper.

By assuming $\psi = \phi - (e_{15}/\Xi_{11})u_3$, Eq. (4) becomes

$$\nabla^2\psi = 0 \tag{14}$$

whose solution is

$$\psi = (B_1e^{-\chi_1 x_2} + B_2e^{\chi_1 x_2})e^{i\omega(t-(x_1/c))} \tag{15}$$

where $\chi_1 = \omega/c$.

Substituting Eq. (4) into Eq. (3) yields

$$\bar{c}_{44}\nabla^2 u_3 = \rho\frac{\partial^2 u_3}{\partial t^2} \tag{16}$$

where $\bar{c}_{44} = c_{44} + (e_{15}^2/\Xi_{11})$, which is stiffened elastic constant in the piezoelectric layer.

The solution of Eq. (16) can be expressed as

$$u_3 = (A_1e^{-\chi_2 x_2} + A_2e^{\chi_2 x_2})e^{i\omega(t-(x_1/c))} \quad \text{if } c < v \tag{17}$$

$$u_3 = (A_1\cos\chi_2 x_2 + A_2\sin\chi_2 x_2)e^{i\omega(t-(x_1/c))} \quad \text{if } v' > c > v \tag{18}$$

where $\chi_2 = \omega/c\sqrt{|1-(c/v)^2|}$ and $v^2 = \bar{c}_{44}/\rho$.

The electric potential can now be obtained from Eqs. (15), (17) and (18),

$$\phi = \left[(B_1e^{-\chi_1 x_2} + B_2e^{\chi_1 x_2}) + \frac{e_{15}}{\Xi_{11}}(A_1e^{-\chi_2 x_2} + A_2e^{\chi_2 x_2})\right]e^{i\omega(t-(x_1/c))} \quad \text{if } c < v \tag{19}$$

$$\phi = \left[(B_1e^{-\chi_1 x_2} + B_2e^{\chi_1 x_2}) + \frac{e_{15}}{\Xi_{11}}(A_1\cos\chi_2 x_2 + A_2\sin\chi_2 x_2)\right]e^{i\omega(t-(x_1/c))} \quad \text{if } v' > c > v \tag{20}$$

The shear stresses in the metal plate can be obtained by substituting Eq. (13) into Eq. (2),

$$\sigma_{23}' = c_{44}'(-\chi' C_1e^{-\chi' x_2} + \chi' C_2e^{\chi' x_2})e^{i\omega(t-(x_1/c))} \tag{21}$$

The shear stress in the piezoelectric layer can be obtained by substituting Eqs. (17)–(20) into Eq. (5),

$$\sigma_{23} = [(-\chi_2)\bar{c}_{44}(A_1e^{-\chi_2 x_2} - A_2e^{\chi_2 x_2}) + (-\chi_1)e_{15}(B_1e^{-\chi_1 x_2} - B_2e^{\chi_1 x_2})]e^{i\omega(t-(x_1/c))} \quad \text{if } c < v \tag{22}$$

$$\sigma_{23} = [(-\chi_2)\bar{c}_{44}(A_1 \sin \chi_2 x_2 - A_2 \cos \chi_2 x_2) + (-\chi_1)e_{15}(B_1 e^{-\chi_1 x_2} - B_2 e^{\chi_1 x_2})]e^{i\omega(t-(x_1/c))} \quad \text{if } v' > c > v \tag{23}$$

The dispersion characteristics of the SH wave by the surface wave solution in this piezoelectric coupled plate will be obtained by studying the general solutions derived above to satisfy the boundary conditions shown in Eqs. (6)–(11).

3. Dispersion relation

Substituting solutions of this piezoelectric coupled plate into the boundary conditions will result in an eigen-value problem from which the dispersive characteristics for this piezoelectric coupled plate may be deduced.

For the case when $c < v$, the boundary conditions in Eqs. (6)–(11) become the following expression after substituting the solutions in Eqs. (13)–(23) in them,

$$C_1 + C_2 = A_1 + A_2 \tag{24}$$

$$(-\chi_2)\bar{c}_{44}(A_1 - A_2) + (-\chi_1)e_{15}(B_1 - B_2) = (-\chi')c'_{44}C_1 + \chi' c'_{44}C_2 \tag{25}$$

$$B_1 + B_2 + \frac{e_{15}}{\Xi_{11}}(A_1 + A_2) = 0 \tag{26}$$

$$(-\chi_2)\bar{c}_{44}(A_1 e^{\chi_2 h} - A_2 e^{-\chi_2 h}) + (-\chi_1)e_{15}\left(B_1 e^{\chi_1 h} - B_2 e^{-\chi_1 h}\right) = 0 \tag{27}$$

$$(B_1 e^{\chi_1 h} + B_2 e^{-\chi_1 h}) + \frac{e_{15}}{\Xi_{11}}\left(A_1 e^{\chi_2 h} + A_2 e^{-\chi_2 h}\right) = 0 \tag{28}$$

$$C_1 e^{-\chi' h'} - C_2 e^{\chi' h'} = 0 \tag{29}$$

From Eq. (29), we have,

$$C_1 = C_2 e^{2\chi' h'} \tag{30}$$

Substituting Eqs. (24) and (30) into Eq. (25) yields,

$$B_1 - B_2 = D_1 A_1 + D_2 A_2 \tag{31}$$

where

$$D_1 = \frac{(e^{2\chi' h'} - 1)}{(e^{2\chi' h'} + 1)} \frac{c'_{44}}{e_{15}} \sqrt{1 - \left(\frac{c}{v'}\right)^2} - \frac{\bar{c}_{44}}{e_{15}} \sqrt{\left|1 - \left(\frac{c}{v}\right)^2\right|},$$

$$D_2 = \frac{(e^{2\chi' h'} - 1)}{(e^{2\chi' h'} + 1)} \frac{c'_{44}}{e_{15}} \sqrt{1 - \left(\frac{c}{v'}\right)^2} + \frac{\bar{c}_{44}}{e_{15}} \sqrt{\left|1 - \left(\frac{c}{v}\right)^2\right|}$$

B_1 and B_2 can be expressed in terms of A_1 and A_2 as follows when taking references of Eqs. (26) and (31)

$$B_1 = \frac{1}{2}\left(D_1 - \frac{e_{15}}{\Xi_{11}}\right)A_1 + \frac{1}{2}\left(D_2 - \frac{e_{15}}{\Xi_{11}}\right)A_2 \tag{32}$$

$$B_2 = \frac{1}{2}\left(-D_1 - \frac{e_{15}}{\Xi_{11}}\right)A_1 + \frac{1}{2}\left(-D_2 - \frac{e_{15}}{\Xi_{11}}\right)A_2 \tag{33}$$

Substituting B_1 and B_2 into Eqs. (27) and (28), we have,

$$E_1A_1 + E_2A_2 = 0 \tag{34}$$

$$E_3A_1 + E_4A_2 = 0 \tag{35}$$

where

$$E_1 = \frac{1}{2}\left(D_1 - \frac{e_{15}}{\Xi_{11}}\right)e^{\chi_1 h} - \frac{1}{2}\left(-D_1 - \frac{e_{15}}{\Xi_{11}}\right)e^{-\chi_1 h} + \frac{1}{2}(D_2 - D_1)e^{\chi_2 h}$$

$$E_2 = \frac{1}{2}\left(D_2 - \frac{e_{15}}{\Xi_{11}}\right)e^{\chi_1 h} - \frac{1}{2}\left(-D_2 - \frac{e_{15}}{\Xi_{11}}\right)e^{-\chi_1 h} - \frac{1}{2}(D_2 - D_1)e^{-\chi_2 h}$$

$$E_3 = \frac{1}{2}\left(D_1 - \frac{e_{15}}{\Xi_{11}}\right)e^{\chi_1 h} + \frac{1}{2}\left(-D_1 - \frac{e_{15}}{\Xi_{11}}\right)e^{-\chi_1 h} + \frac{e_{15}}{\Xi_{11}}e^{\chi_2 h}$$

$$E_4 = \frac{1}{2}\left(D_2 - \frac{e_{15}}{\Xi_{11}}\right)e^{\chi_1 h} + \frac{1}{2}\left(-D_2 - \frac{e_{15}}{\Xi_{11}}\right)e^{-\chi_1 h} + \frac{e_{15}}{\Xi_{11}}e^{-\chi_2 h}$$

The dispersive relation can be obtained by imposing the condition for non-trivial solution of A_1 and A_2, namely,

$$\begin{vmatrix} E_1 & E_2 \\ E_3 & E_4 \end{vmatrix} = 0 \tag{36}$$

i.e.

$$E_1E_4 - E_2E_3 = 0 \tag{37}$$

For the case when $v' > c > v$, the following equations will be obtained after substituting the solutions in Eqs. (13)–(23) into boundary conditions Eqs. (6)–(11)

$$C_1 + C_2 = A_1 \tag{38}$$

$$(-\chi_2)\bar{c}_{44}(-A_2) + (-\chi_1)e_{15}(B_1 - B_2) = (-\chi')c'_{44}C_1 + \chi' c'_{44}C_2 \tag{39}$$

$$B_1 + B_2 + \frac{e_{15}}{\Xi_{11}}(A_1) = 0 \tag{40}$$

$$(-\chi_2)\bar{c}_{44}(-A_1\sin\chi_2 h - A_2\cos\chi_2 h) + (-\chi_1)e_{15}(B_1e^{\chi_1 h} - B_2e^{-\chi_1 h}) = 0 \tag{41}$$

$$\left(B_1e^{\chi_1 h} + B_2e^{-\chi_1 h}\right) + \frac{e_{15}}{\Xi_{11}}(A_1\cos\chi_2 h - A_2\sin\chi_2 h) = 0 \tag{42}$$

and Eq. (29) remains same.

Similarly, B_1 and B_2 can be expressed in terms of A_1 and A_2 as

$$B_1 = \frac{1}{2}\left(\frac{1}{2}(D_1 + D_2) - \frac{e_{15}}{\Xi_{11}}\right)A_1 + \frac{1}{4}(D_2 - D_1)A_2 \tag{43}$$

$$B_2 = \frac{1}{2}\left(-\frac{1}{2}(D_1 + D_2) - \frac{e_{15}}{\Xi_{11}}\right)A_1 - \frac{1}{4}(D_2 - D_1)A_2 \tag{44}$$

Substituting B_1 and B_2 into Eqs. (41) and (42), we have

$$E_5A_1 + E_6A_2 = 0 \tag{45}$$

$$E_7A_1 + E_8A_2 = 0 \tag{46}$$

where

$$E_5 = \frac{1}{2}\left(\frac{1}{2}(D_1+D_2) - \frac{e_{15}}{\Xi_{11}}\right)e^{\chi_1 h} - \frac{1}{2}\left(-\frac{1}{2}(D_1+D_2) - \frac{e_{15}}{\Xi_{11}}\right)e^{-\chi_1 h} - \frac{1}{2}(D_2-D_1)\sin\chi_2 h$$

$$E_6 = \frac{1}{2}(D_2-D_1)\left(\frac{1}{2}e^{\chi_1 h} + \frac{1}{2}e^{-\chi_1 h} - \cos\chi_2 h\right)$$

$$E_7 = \frac{1}{2}\left(\frac{1}{2}(D_1+D_2) - \frac{e_{15}}{\Xi_{11}}\right)e^{\chi_1 h} + \frac{1}{2}\left(-\frac{1}{2}(D_1+D_2) - \frac{e_{15}}{\Xi_{11}}\right)e^{-\chi_1 h} + \frac{e_{15}}{\Xi_{11}}\cos\chi_2 h$$

$$E_8 = \frac{1}{2}(D_2-D_1)\left(\frac{1}{2}e^{\chi_1 h} - \frac{1}{2}e^{-\chi_1 h} - \frac{e_{15}}{\Xi_{11}}\sin\chi_2 h\right)$$

The dispersive relation can then be obtained as follows

$$\begin{vmatrix} E_5 & E_6 \\ E_7 & E_8 \end{vmatrix} = 0 \tag{47}$$

i.e.

$$E_5E_8 - E_6E_7 = 0 \tag{48}$$

4. Mode shapes in piezoelectric layer

The mode shapes for deflection and electric potential in the thickness direction of piezoelectric layer may be obtained from characteristic equation of Eq. (37) or (48) depending on the wave velocity as follows.

When $c < v$, Eq. (34) implies

$$A_2 = -\frac{E_1}{E_2}A_1 \tag{49}$$

and the spatial components of the deflection u_3 and the electric potential ϕ in x_2-direction are from Eqs. (17) and (19)

$$\bar{u}_3 = A_1\left(e^{-\chi_2 x_2} - \frac{E_1}{E_2}e^{\chi_2 x_2}\right) \tag{50}$$

$$\begin{aligned}\bar{\phi} = {} & A_1\left[\frac{1}{2}\left(D_1 - \frac{e_{15}}{\Xi_{11}}\right) - \frac{1}{2}\left(D_2 - \frac{e_{15}}{\Xi_{11}}\right)\frac{E_1}{E_2} + \frac{e_{15}}{\Xi_{11}}\right]e^{-\chi_2 x_2} \\ & + A_1\left[\frac{1}{2}\left(-D_1 - \frac{e_{15}}{\Xi_{11}}\right) - \frac{1}{2}\left(-D_2 - \frac{e_{15}}{\Xi_{11}}\right)\frac{E_1}{E_2} - \frac{e_{15}}{\Xi_{11}}\frac{E_1}{E_2}\right]e^{\chi_2 x_2}\end{aligned} \tag{51}$$

The mode shapes for deflection of the metal core is obtained from Eq. (13),

$$\bar{u}_3' = C_2(e^{-\chi' x_2}e^{2\chi' h'} + e^{\chi' x_2}) \tag{52}$$

When $v' > c > v$, Eq. (45) gives

$$A_2 = -\frac{E_5}{E_6}A_1 \tag{53}$$

and the spatial components of the deflection u_3 and the electric potential ϕ in x_2-direction are

$$\bar{u}_3 = A_1\left(\cos\chi_2 x_2 - \frac{E_5}{E_6}\sin\chi_2 x_2\right) \tag{54}$$

$$\bar{\phi} = A_1\left[\frac{1}{2}\left(\frac{1}{2}(D_1+D_2)-\frac{e_{15}}{\Xi_{11}}\right)-\frac{1}{4}(D_2-D_1)\frac{E_5}{E_6}\right]e^{-\chi_2 x_2} + A_1\left[\frac{1}{2}\left(-\frac{1}{2}(D_1+D_2)-\frac{e_{15}}{\Xi_{11}}\right)+\frac{1}{4}(D_2-D_1)\frac{E_5}{E_6}\right]e^{\chi_2 x_2} + A_1\frac{e_{15}}{\Xi_{11}}\left(\cos\chi_2 x_2 - \frac{E_5}{E_6}\sin\chi_2 x_2\right) \quad (55)$$

Numerical simulations are performed to illustrate the results of the dispersive characteristics and the mode shapes obtained above and presented in the following section.

5. Numerical simulations and discussions

In this numerical session, SH wave propagation in a steel core plate surface bonded by a layer of PZT 4 will be discussed. In Table 1, the material properties of steel and PZT 4 are listed. The shear wave velocities for the host steel and the PZT layer are $v'|_{\text{steel}} = 3281$ m/s, $v|_{\text{PZT4}} = 2351$ m/s. The Bleustein–Gulyayev surface wave velocities in PZT4 can be determined (Viktorov, 1981; Gulyaev and Plesskii, 1977; Bleustein, 1969) by the following equation $v_{\text{B}} = v(1-(k_{15}^4/(1+k_{15}^2)^2))^{1/2}$, and $k_{15}^2 = e_{15}^2/c_{44}\Xi_{11}v$ is the shear wave velocity of the piezoelectric material. Such surface wave velocity of PZT4 is $v_{\text{B}}|_{\text{PZT4}} = 2181$ m/s.

The non-dimensional phase velocity is taken as $\bar{c} = c/c_{\text{B}}$ and the non-dimensional wave number is used by $\bar{\xi} = \xi h/2\pi$. In Fig. 2, the dispersion curves for the first three modes of the steel–PZT coupled plate are presented. It is observed that the phase velocity of the first mode approaches the Bleustein–Gulyaev wave velocity at large wave number. This is due to the fact the surface wave for the piezoelectric layer becomes dominant when the wave number is large compared with the thickness of the layer for this type of the surface wave solution for the piezoelectric layer. Another observation from Fig. 2 is that the wave velocities of the higher modes, i.e. second and third modes, tend to the shear velocity of the piezoelectric layer at higher wave number.

In order to give comparison of the dispersion characteristics by the piezoelectric effects, Fig. 3 presents the dispersion curves for the first mode at different ratios of the thickness of the piezoelectric layer to the thickness of the host plate. The solution of wave propagation in a semi-infinite steel–PZT 4 piezoelectric coupled medium discussed by Wang et al. (2001) is used here as the benchmark for the case of zero ratio of the thickness of the piezoelectric layer. Big discrepancy is found at lower wave number. However, all the curves convergence at higher wave number. This observation is within the expectation. At the lower ratios, the wavelength of the SH wave is comparable with the thickness of the layer, thus the dispersions curves show different variations for different thickness ratios of the thickness of the layer. Besides, the wave velocities at smaller ratios are bigger than those for higher wave number as the steel core is stiffer than the piezoelectric layer. Nevertheless, since the wavelength of the SH wave is smaller than the thickness of the

Table 1
Material properties

	Host structure (steel)	Piezoelectric layer (PZT4)
Young's module (N/m^2)	$E = 210\times10^9$	$c_{11} = 132\times10^9$ $c_{12} = 73\times10^9$ $c_{22} = 115\times10^9$ $c_{13} = 71\times10^9$
Mass density (kg/m^3)	7.8×10^3	7.5×10^3
e_{15} (C/m^2)	–	10.5
e_{31} (C/m^2)	–	−4.1
Ξ_0 (F/m)	–	8.854×10^{-12}
Ξ_{11}/Ξ_0	–	800
Ξ_{33}/Ξ_0	–	660

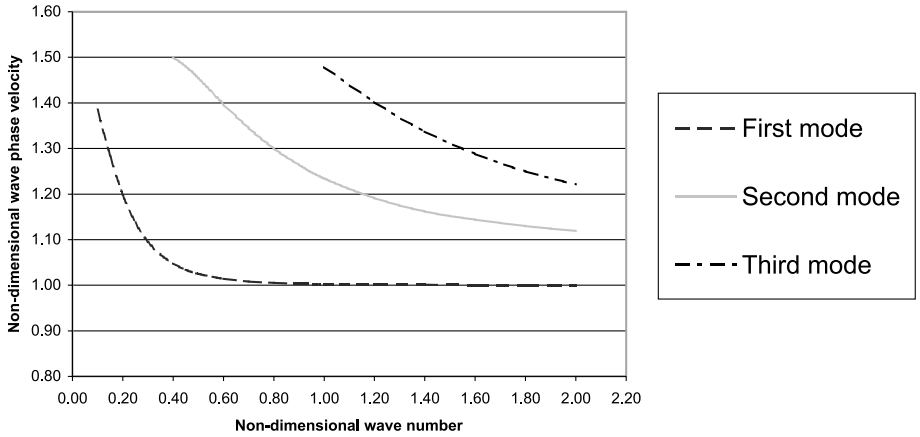

Fig. 2. Dispersions curves for steel-PZT plate.

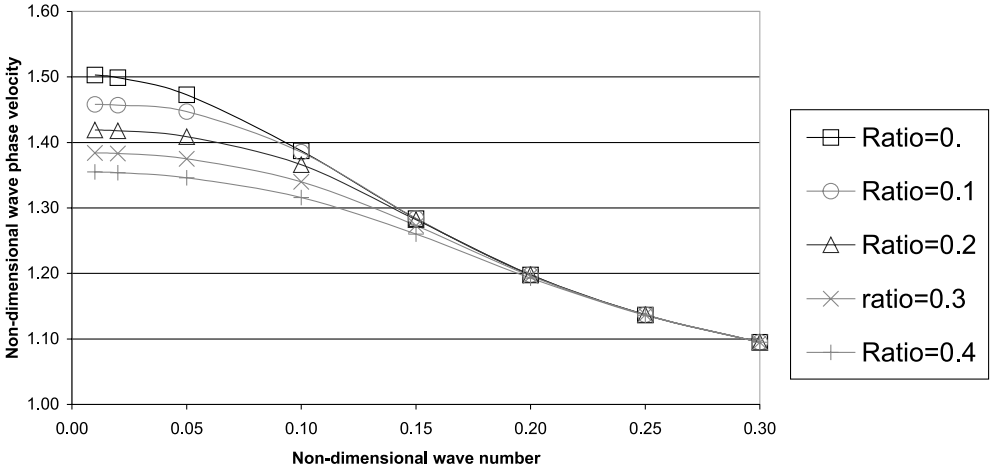

Fig. 3. Comparison of the first wave mode for different ratios of the thickness of piezoelectric layer.

piezoelectric layer at higher wave number, the piezoelectric layer dominates the characteristics of the SH wave propagation. Hence the asymptotic solution of the wave velocity for this first mode is no doubt the Bleustein–Gulyaev wave velocity shown in Figs. 2 and 3.

The mode shapes of the deflection and the electric potential in the thickness direction of the piezoelectric layer are presented in Figs. 4–6 for the first mode shape at non-dimensional wave number of 0.1 and 1.0 and the second mode shape at non-dimensional wave number of 1.0 separately. Similar to the recent results obtained by Wang et al. (2001), the electric potential changes its shape from an approximate quadratic shape for the first mode and at lower wave number, 0.1, to a distorted one for the same mode but at higher wave number, i.e. 1.0. In addition, this distorted shape changes to a more distorted shape with one more zero nodes for the second mode at the same wave number 1.0. The mode shape for the deflection changes its shape from a straight line to a skewed one and finally to a curve with one zero node when the first and second mode shape are studied at wave number of 0.1 and 1.0.

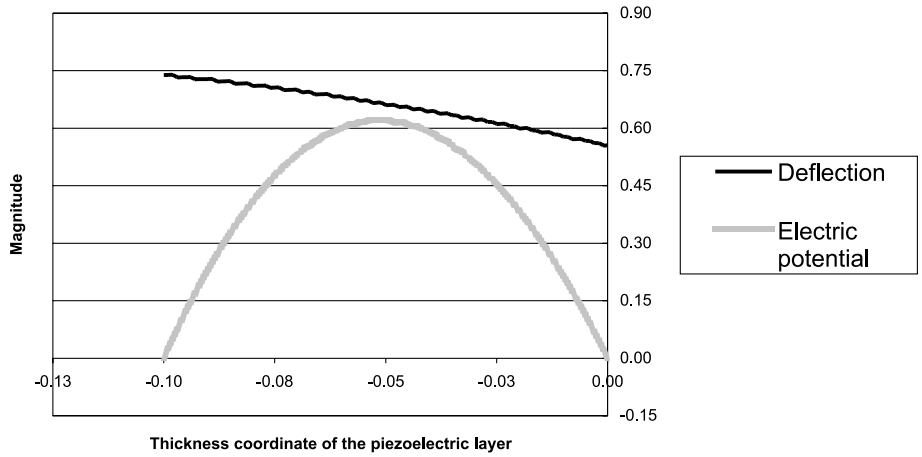

Fig. 4. First mode shape of the piezoelectric layer at non-dimensional wave number 0.1.

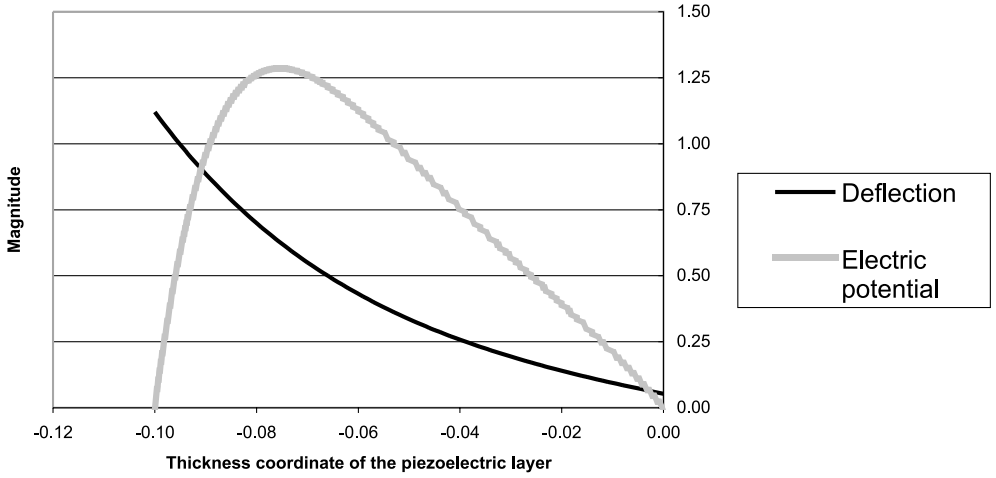

Fig. 5. First mode shape of the piezoelectric layer at non-dimensional wave number 1.0.

6. Concluding remarks

This paper is the first part of the study on the SH wave propagation in the piezoelectric coupled plate by use of IDT. In this part, the dispersion characteristics of the wave, as well as the mode shapes of the deflection and the electric potential of the piezoelectric layer are presented based on the type of surface wave solution. From the numerical simulation of a steel–PZT coupled plate structure, the Bleustein–Gulyayev surface wave is found for the first mode of this SH wave propagation. Besides, the asymptotic solution for higher wave modes is found to be the shear wave velocity of the piezoelectric layer. The comparison of the dispersion curves for different ratios of the piezoelectric thickness is also conducted. The result of the surface wave propagation in a semi-infinite piezoelectric coupled medium is used as the zero ratio of the thickness of the piezoelectric layer for the comparison. The mode shapes of the deflection and the electric

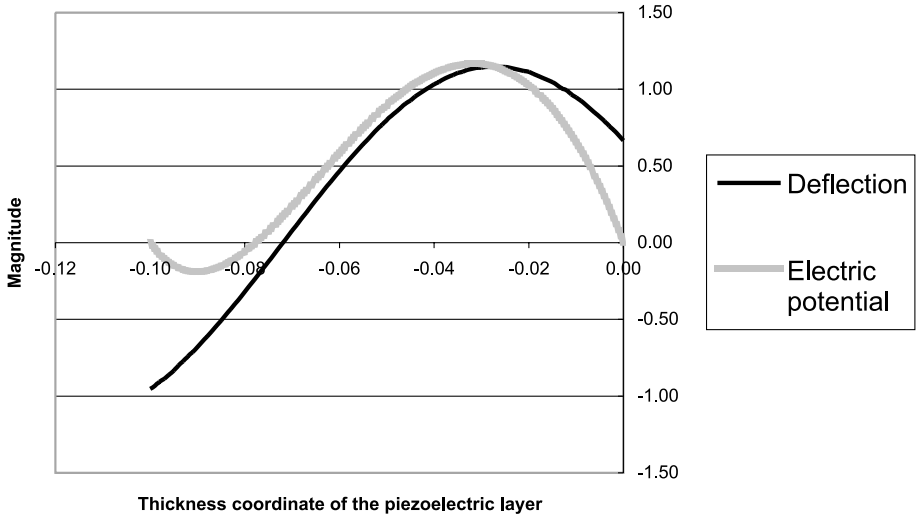

Fig. 6. Second mode shape of the piezoelectric layer at non-dimensional wave number 1.0.

potential of the piezoelectric layer are also derived, and the variation of the mode shapes shows a trend of standard shapes to distorted shapes with more zero nodes for higher modes and at higher wave number. This research provides the basic model for the analysis of the wave propagation in piezoelectric coupled plate. In second part of the research, this type of surface wave solution will be used for the study of the wave excitation by use of IDT.

References

Auld, B.A., 1973a. In: Acoustic Fields and Waves in Solids, vol. I. Wiley, New York.

Auld, B.A., 1973b. In: Acoustic Fields and Waves in Solids, vol. II. Wiley, New York.

Badcock, R.A., Birt, E.A., 2000. The use of 0–3 piezocomposite embedded Lamb wave sensors for detection of damage in advanced fibre composites. Smart Materials and Structures 9, 291–297.

Bleustein, J.L., 1969. Some simple modes of wave propagation in an infinite piezoelectric plates. Journal of Acoustics Society of America 45, 614–620.

Campbell, C.K., 1998. Surface Acoustic Wave Devices for Mobile and Wireless Communications. Academic Press, New York.

Curtis, R.G., Redwood, M., 1973. Transverse surface waves on a piezoelectric material carrying a metal layer of finite thickness. Journal of Applied Physics 44, 2002–2007.

Graff, K.F., 1975. Wave motion in elastic solids. Dover Publications, INC., New York.

Gulyaev, Y.V., Plesskii, V.P., 1977. Gap acoustic waves in piezoelectric materials. Akust. Zhurn. 23, 716–723.

Hanhua, F., Xingjiao, L., 1991. Shear-horizontal surface waves in the layered structure. In: Ultrasonics Symposium, pp. 415–418.

Hanhua, F., Xingjiao, L., 1993. Shear-horizontal surface waves in a layered structure of piezoelectric ceramics. IEEE Transactions on Ultrasonics, Ferroelectrics, and Frequency Control 40, 167–170.

Kielczynski, P.J., Pajewski, W., Szalewski, M., 1989. Shear-horizontal surface waves on piezoelectric ceramics with depolarised surface layer. IEEE Transactions on Ultrasonics, Ferroelectrics, and Frequency Control 36, 287–293.

Monkhouse, R.S.C., Wilcox, P.W., Dalton, R.P., Cawley, P., 2000. The rapid monitoring of structures using interdigital Lamb wave transducers. Smart Materials and Structures 9, 304–309.

Morgan, D.P., 1998. History of SAW devices. In: IEEE International Frequency Control Symposium, pp. 439–460.

Parton, V.Z., Kudryavtser, B.A., 1988. Electromagnetoelasticity. Gordon and Breach Science Publishers, New York.

Sun, C.T., Cheng, N.C., 1974. Piezoelectric waves on a layered cylinder. Journal of Applied Physics 45, 4288–4294.

Varadan, V.K., Varadan, V.V., 2000. Microsensors, microelectromechanical systems (MEMS), and electronics for smart structures and systems. Smart Materials and Structures 9, 953–972.

Viktorov, I.A., 1981. Surface Waves in Solids. Nauka, Moscow (in Russian).

Wang, Q., Quek, S.T., Varadan, V.K., 2001. Love wave propagation in piezoelectric coupled media. Smart Materials and Structures 10, 380–388.

White, R.M., 1998. Acoustic sensors for physical, chemical, and biochemical application. In: IEEE International Frequency Control Symposium, pp. 587–594.